Available online at www.sciencedirect.com
ScienceDirect
Journal of the European Ceramic Society 31 (2011) 485–492
www.elsevier.com/locate/jeurceramsoc

Wear resistance glass-ceramics with a gahnite phase obtained in $CaO\text{-}MgO\text{-}ZnO\text{-}Al_2O_3\text{-}B_2O_3\text{-}SiO_2$ system

Daniela Herman *, Tomasz Okupski, Wiesław Walkowiak

Koszalin University of Technology, Racławicka 15-17, 75-620 Koszalin, Poland

Received 14 May 2010; received in revised form 7 October 2010; accepted 12 October 2010
Available online 26 November 2010

Abstract

The thermal conditions for obtaining the glass-ceramic material of $Al_{0.107}B_{0.374}Mg_{0.043}Zn_{0.282}Ca_{0.100}Si_{0.927}O_3$ with a crystalline phase in the form of gahnite ($ZnAl_2O_4$) were specified. The activation energy E_a and the Avrami parameter n for the crystallisation process were determined with the non-isothermal DTA procedure. The maximum temperatures of crystallisation of phases, depending on the rate of heating, ranged between 800–840 °C for willemite and 870–915 °C for gahnite. The homogeneous crystalline spinel phase was obtained by heat treatment above 1000 °C. Precipitation solely of a ghanite phase from glass-ceramic causes a relative increase in its fracture toughness and wear resistance compared to the two-phase materials, i.e., $K_{IC} = 2.12\text{–}1.65\ MPam^{1/2}$ and $w_s = 0.21 \times 10^{-4}\ mm^3/Nm$ to $w_s = 1.43 \times 10^{-4}\ mm^3/Nm$.

Keywords: Glass ceramics; Spinels; Wear resistance

1. Introduction

In recent years there has been an exciting development of technologies and applications of glass-ceramic materials. This is due to the fact that these materials exhibit a unique potential for the combination of their properties with the result that they can be designed for specific applications: body stubs in microelectronics, biomaterials, composites fillers, binders, highly durable and hard wear resistant materials.[1,2] The desired properties of glass-ceramic materials were obtained for the application of the appropriate chemical composition of initial glass, a nucleation system and crystallisation conditions.

Glasses, which form the initial material for the manufacture of glass-ceramics are more vulnerable to flaws and cracks, which is expressed in their low resistance to brittle fracture, i.e. about $1\ MPam^{1/2}$. After processing glass into glass-ceramic material, K_{IC} usually increases ($1\text{–}2.5\ MPam^{1/2}$).[3] By the precipitation of crystalline phases, which are much harder or "crush" more easily (due to the introduction of areas absorbing the fracture energy), it is possible to reduce the sensitivity of glass-ceramic materials to flaws.

Furthermore, the ability to manipulate the microstructure of such materials allows a correlation with its many properties, in particular tribological ones. Owing to that, the problems with the selection of such materials that are resistant to wear can be increasingly easily solved. Among vitreous systems developed whose purpose is to obtain the specified crystalline phases that enhance the mechanical properties, there is a growing interest in $CaO\text{-}MgO\text{-}Al_2O_3\text{-}SiO_2$ systems, where the main crystalline phase is diopside.[4–6] By controlling the size of crystals of diopside in plastic material, a significant increase in hardness and wear resistance for the benefit of the fine-crystalline structure was obtained.[7] In similar systems, where next to diopside wollastonite was crystallised, those materials in which the content of diopside was higher were marked with the high abrasive-wear coefficient $w_s = 10^{-3}\text{–}10^{-4}\ mm^3/Nm$[8]; however, the presence of a wollastonite phase is more favourable in materials for use in dentistry, that are known as A–W ceramics. The glass-ceramic materials from an apatite–wollastonite (AW) phase are obtainable in the system of $MgO\text{-}CaO\text{-}SiO_2\text{-}Pa_2O_5\text{-}F$, for which the abrasive-wear coefficient was $w_s = 0.9\text{–}1.8 \times 10^{-4}\ mm^3/Nm$[9]; however, a higher abrasive-wear resistance $w_s = 10^{-4}\text{–}10^{-5}\ mm^3/Nm$ was displayed by the material from the system of $K_2O\text{-}B_2O_3\text{-}Al_2O_3\text{-}SiO_2\text{-}MgO$-

* Corresponding author.
E-mail addresses: daniela.herman@tu.koszalin.pl, danher@poczta.onlet.pl (D. Herman), tomasz.okupski@tu.koszalin.pl (T. Okupski), wieslaw.walkowiak@tu.koszalin.pl (W. Walkowiak).

0955-2219/$ – see front matter © 2010 Elsevier Ltd. All rights reserved.
doi:10.1016/j.jeurceramsoc.2010.10.021

F with an addition of mica that also has applications in dentistry.[10]

The high resistance to wear and the brittle fracture of glass-ceramics materials is also used to strengthen composites, both dense and porous.[11–13] The main crystalline phase in the form of diopside is very widely used in dense composites. Compared to other reinforcing phases, diopside has the advantage that it has relatively low production costs in comparison with other materials, and it also contributes to a reduction of the sintering temperature. Composites Al_2O_3 with an addition of 3% diopside have better mechanical properties than those without its participation, $K_{IC} = 5.2–4.1$ MPam$^{1/2}$ and the abrasive-wear coefficient $w_s = 10^{-16}–10^{-15}$ mm^3/Nm, respectively.[14]

As opposed to the dense composites, the glass-crystalline material in the porous abrasive composites (bonded abrasive tools) must be considered as a liquid meniscus in the firing temperature, maintaining abrasive grains together by the action of surface tension forces, creating the so-called bond bridges. The formation of bridges and bonds with grains results from the binder spreading on grain surfaces and physico-chemical interaction with them. The system obtained of bridges involving abrasive grains determines the ultimate strength of the abrasive composite. For this reason, among others in current technological solutions, the process of sintering of such systems takes place mainly with classical silicate glass adhesives.[15,16] A growing demand for special tools, e.g. for machining ductile alloys,[17] inspires the search for new technological solutions. Designs for attractive binding systems are dictated by the need to open a composite structure, i.e. to increase their porosity, which simultaneously involves an increase in mechanical properties of adhesives.[18–20]

In addition, an exciting development in technology of submicrocrystalline abrasive particles[21,22] leads to changes in the approach to the design of ceramic bonds. Submicrocrystalline abrasive grains of alumina type SG with the abrasive-wear coefficient of $w_s = 1.86 \pm 0.4 \times 10^{-7}$ mm^3/Nm reached almost twice the fracture toughness compared to the widely used grains of fused alumina.[23] Thus, more durable grains and composites with higher porosity will require the use of binders with a higher fracture toughness and resistance to abrasive wear than the amorphous binder. By replacing glass adhesives, whose wear resistances are relatively low, $w_s = 2.5 \times 10^{-3}$ mm^3/Nm,[24] with materials that have different microstructural characteristics and different types of crystalline phases, it will be possible to limit the propagation of cracks in the binder. The experimental investigations described in this paper are aimed at developing a glass-ceramic material that functions as a bonding material in porous composites with a level of fracture toughness being sufficient to maintain its abrasive wear in a dynamic equilibrium with the progressive wear of abrasive grains, thereby reducing the abrasive wear of grinding wheels.

2. Experimental procedure

Glass-ceramics of the chemical formula of $Al_{0.107}B_{0.374}Mg_{0.043}Zn_{0.282}Ca_{0.100}$ $Si_{0.927}O_3$ were obtained through the application of a typical technology from glass-making industry. The raw material in the form of H_3BO_3, $CaCO_3$, $MgCO_3$, $Al(OH)_3$, SiO_2 and ZnO was melted in the air at the temperature of 1500 °C for 2 h. The molten frit was rapidly cooled down in water and dried. Then, this frit was powdered in a ball grinder until the fraction below 63 μm was obtained. The crystallisability of the material was determined with a DTA method using a thermal analyser manufactured by MOM (Hungary) adapted to work in the air with the ambient temperature up to 1273 K. A powdered specimen of 0.8 g in weight was placed in a crucible, using also corundum as a reference material. To observe the microstructure and test the mechanical properties, the obtained powder was formed into shapes φ15 mm × 10 mm in dimension and thermally processed under conditions corresponding to the maximum nucleation temperature, in accordance with DTA data, i.e. 920 °C and at the temperature allowing the abrasive grains of aluminium oxide type SG80 Norton's to be bonded into porous abrasive composite, i.e. 1100 °C. The decomposition of superimposed exothermal effects was developed using Origin 6.0 software with the Lorentz's method. The specimens processed thermally as above were polished to obtain a bright polish and were then subjected to hardness, fracture toughness and tribological tests. The hardness test and the measurements of crack lengths were carried out using a Vickers-Hardness Tester FV-700 manufactured by Future–Tech. Corp. (Japan). The load range was 1–30 N, the measurement time 10 s (ranging 1–99 s), and the electronic measurement accuracy was up to 0.1 μm. An X-ray phase analysis was carried out on a SIEMENS D 5000 apparatus using CuK radiation; counting time 5 s, specimen rotation [RPM] 1 s, measuring range 10–60 s. The microstructure of materials undergoing the heat treatment and the etching process at 10% HF solution was examined with SEM with a JEOL-JSM-5500 LX (Japan) instrument. The wear rate coefficient w_s was determined using a T-01M tribotester of a Ball-on-Disk type. The counterspecimen was a ball made of 100Cr6 steel (dia. 10 mm, 62 ± 2HRC), a load at frictional contact $F = 10$ N, linear sliding speed $v = 0.3$ m/s, total sliding length $s = 1000$ m, friction radius $r_t = 7$ mm. The profiles of worn grooves while testing were measured using a Hommel-TesterT 2000 profilometer. The volume of worn material V was calculated as a product of the average cross-sectional area of wear and the friction radius r_t. The wear rate coefficient w_s (mm^3/Nm) of the materials under investigation is then given by expression $w_s = V/F \times S$, where V is the volume of the material worn [mm^3], F is load [N] and S is sliding length [m].

3. Results and discussion

3.1. Crystallisation kinetics and X-ray diffraction phase analysis

The activation energy for the crystallisation of an $Al_{0.107}B_{0.374}Mg_{0.043}Zn_{0.282}Ca_{0.100}Si_{0.927}O_3$ system was determined with the non-isothermal method, where the characteristics of a crystallisation peak determined with DTA were monitored as a function of the heating rate and the temperature (Fig. 1).

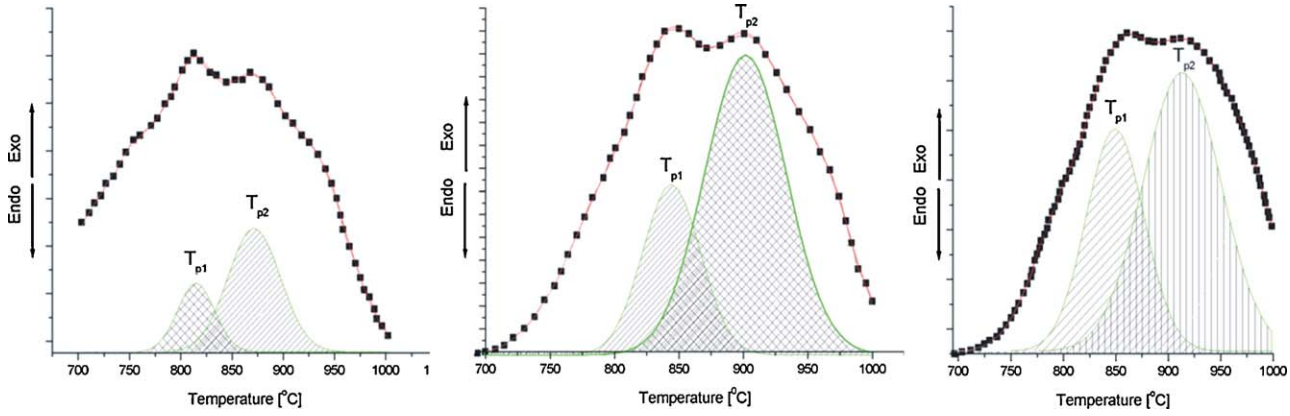

Fig. 1. DTA curves for material under investigation at different heating rates.

Testing was carried out with the use of a modified Kissinger's method considering that the crystallisation mechanism such as volumetric crystallisation or surface crystallisation should be expected to obtain the correct activation energies, according to formula[25]:

$$\ln\left(\frac{\beta^n}{T_p^2}\right) = -\frac{mE}{RT} + const \quad (1)$$

where n is the Avrami parameter, connected with a crystallisation mechanism, m represents a dimension of the crystal growth.

The diagram $\ln(T_p^2/\beta^n)$ as a function of $1/T_p$ gives a straight line, and a slope takes the value $(m/n) \times E$. This diagram is known as 'a modified Kissinger-type diagram' (Fig. 2).

To obtain the activation energy for the crystal growth from a modified Kissinger-type diagram, one should know the mechanism of the crystallisation, i.e. the m/n ratio. The Avrami parameter n can be determined by solving Augis-Benett's formula.[26]

$$n = \left(\frac{2.5}{\Delta T}\right)\left(\frac{T_p^2 R}{E_c}\right) \quad (2)$$

where ΔT is the width of the peak at half height.

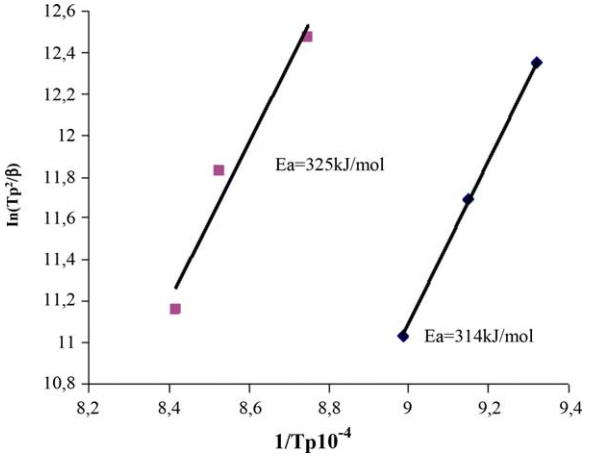

Fig. 2. Dependence of $\ln T_p^2/\beta$ on $1/T_p$ that characterises the activation energy of the material under investigation.

It results from calculations (Table 1) that parameter $n \approx 1$, which attests the mechanism of surface crystallisation.

For special cases $m = n = 1$,[27] where the value determined of the activation energy for the first exothermal peak was 325 kJ/mol and the second peak was 314 kJ/mol, respectively.

An almost simultaneous crystallisation of both phases (a shift at the beginning of DTA curves for about 50 °C) may result from the phase separation (Fig. 3) in microregions enriched with Al^{3+} and Si^{4+}.

This process is significantly marked with the competition of rigid ions in attracting and bonding the oxygen ions ($\varphi Si^{4+} = 9.55$, against $\varphi Al^{3+} = 5.88$). Therefore, willemite predominated at the first stage of treatment (Fig. 3a); however, the crystallisation of gahnite proceeded as a growing batch of glass appeared, which was confirmed by a distinct formation of gahnite crystals inside a vitreous phase (Fig. 3b). Willemite disappeared (Fig. 3c) as the temperature of the thermal treatment was increasing and gahnite formed the main crystalline phase in the proposed material, which was confirmed by XRD analyses (Fig. 4).

A similar mechanism of the gahnite crystal growth was found in a $CaO\text{-}MgO\text{-}K_2O\text{-}Na_2O\text{-}Al_2O_3\text{-}SiO_2$ system.[28] However, gahnite in the case of $ZnO\text{-}Al_2O_3\text{-}SiO_2$ systems with TiO_2, ZrO_2 nucleators is produced by means of two simultaneously proceeding mechanisms: the growth on nucleators distributed in the whole glass and the aluminosilicate solid solutions with a high-quartz structure on the surface of glass particles, thus they are precursors for gahnite, for which the activation energy for the crystallisation with a TiO_2 nucleator is estimated at 344 kJ/mol.[29]

The papers presented previously emphasised the significance of crystallisation catalysts playing an important part in the phase transition and the development of the glass-ceramics texture. By introducing the nucleators of crystallisation in the form of Cr_2O_3, TiO_2 and ZrO_2 to e.g. a $Li_2O\text{-}ZnO\text{-}MgO\text{-}Al_2O_3\text{-}SiO_2$ system, it was possible to obtain among others a gahnite phase in this system. However, beside a $ZnAl_2O_4$ gahnite phase, there were produced virgilite (β quartz ss $Li_xAl_xSi_{3-x}O_6$), lithium aluminosilicate $LiAl(Si_2O_6)$ (pyroxene) and enstatyte $Mg[Si_2O_6]$.[30]

Table 1
Temperatures at maximum of crystallisation peaks depending on a heating rate and a parameter connected with a mechanism of crystallisation.

Heating rate β [°C/min]	T_{p1}		Avrami parameter $n \approx 1$	T_{p2}		Avrami parameter $n \approx 1$
	°C	K		°C	K	
5	800	1073	1.746	870	1143	1.386
10	820	1093	1.223	900	1173	1.011
20	840	1113	1.239	915	1188	1.025

But the occurrence of several crystalline phases from the perspective of the expected high mechanical properties, including tribological ones, is not a favourable phenomenon due to a high probability of a thermo-mechanical stress concentration in interphase boundaries.

3.2. Tribological behaviour: wear rate of glass-ceramics

3.2.1. Mechanical properties. Fracture toughness and wear rate coefficient

The phase composition of the materials under design is changing as a function of heat-treatment parameters, which has a significant influence on their hardness and fracture toughness (Table 2).

Through the heat treatment of the materials under investigations in the area of the first crystallisation peak with gahnite and willemite phases, it is possible to obtain a material with $H_v = 6.86$ GPa and $K_{IC} = 1.65$ MPam$^{1/2}$. A decrease in the phase of willemite and an increase in the phase of gahnite (heat treatment in the area of the second crystallisation peak) brings about an increase in $H_v = 8.37$ GPa and $K_{IC} = 1.93$ MPam$^{1/2}$ as well. A further rise in the temperature of the material's heat treatment up to 1100 °C, where it is possible to use it as binder, i.e. satisfying a condition of wetting the abrasive grains, brings about a further reduction of willemite and a formation of mainly gahnite, which contributes to a further increase in hardness to 8.83 GPa and fracture toughness $K_{IC} = 2.12$ MPam$^{1/2}$.

The proposed material is intended for operation under heavy-duty thermal-mechanical conditions, and in this connection it would be subjected to a gradual wear. The reasons for wear are mostly mechanical in nature; very seldom they are mechanical and connected with the chemical effects of the surrounding environment. An important factor when wear is considered, i.e. for the determination of coefficient w_s, is the hardness and the fracture toughness of co-acting materials. In the case of a larger difference in hardness and K_{IC}, beside an adhesive wear, the abrasive wear may predominate, and then grooves are gouged on the surface of a less hard material (Fig. 5a).

Along with a decrease of K_{IC}, the sub-surface cracks parallel to the surface were developed more easily, which is the reason for a heavier wear by delamination and spalling of the material. These cracks were created to a larger extent in the material of the lowest fracture toughness, where the larger content of a willemite phase was observed ($K_{IC} = 1.65$ MPam$^{1/2}$). Therefore, the relative resistance to an abrasive wear of the materials under investigation depends on a mutual fraction of a spinel phase and monoinosilicate (Fig. 4). A microstructural factor is also here of a great importance: a more uniform structure, despite that a significant increase in an average size of crystallites was observed, exerts a beneficial influence on a rise in the wear resistance. The hardness, fracture toughness and wear resistance as well are relative to the formation of gahnite crystals of a high hardness (8.5 on the Mohs scale), which in the system under investigation comprises the main crystalline phase (Figs. 4d and 6c, Table 2).

The reason for worse properties of the other materials is the occurrence of willemite, a phase of a lower hardness, i.e. 5.5 on the Mohs scale. So far in this system (CMAS), but along with a ZrO_2 nucleator, there were obtained glass-ceramics with the participation of three crystalline phases: gahnite, zinc silicate and zirconium silicate of an average crystal size 5–10 μm. The hardness H_v tested under similar conditions as in the present work was 617–651 kG/mm.[21] However, by introducing nucleators in the form of Cr_2O_3, TiO_2 and ZrO_2 into a similar glass forming system, higher values of hardness, i.e. 738–790 kG/mm^2 were obtained.[1] In this case, the effect of the mechanical cracking of grains or the delamination of tribofilms on a scale corresponding to the size of crystallite grains is likely to be a predominant mechanism of wear. A wear rate as a result of such a mechanism

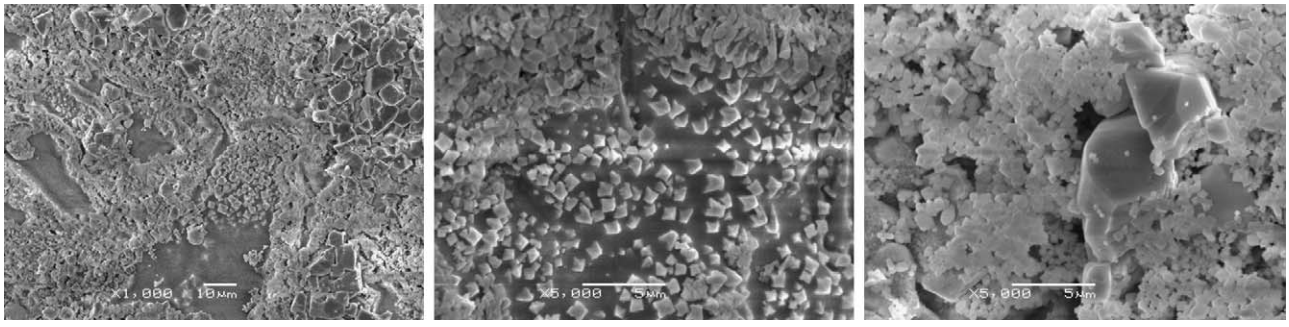

Fig. 3. Microstructure of glass-ceramics at different phases of the process of crystallisation: (a) separation of phases—$T = 800$ °C, (b) spinel precipitation from an amorphous phase—$T = 840$ °C, and (c) an example of willemite disintegration (large crystals)—$T = 1000$ °C.

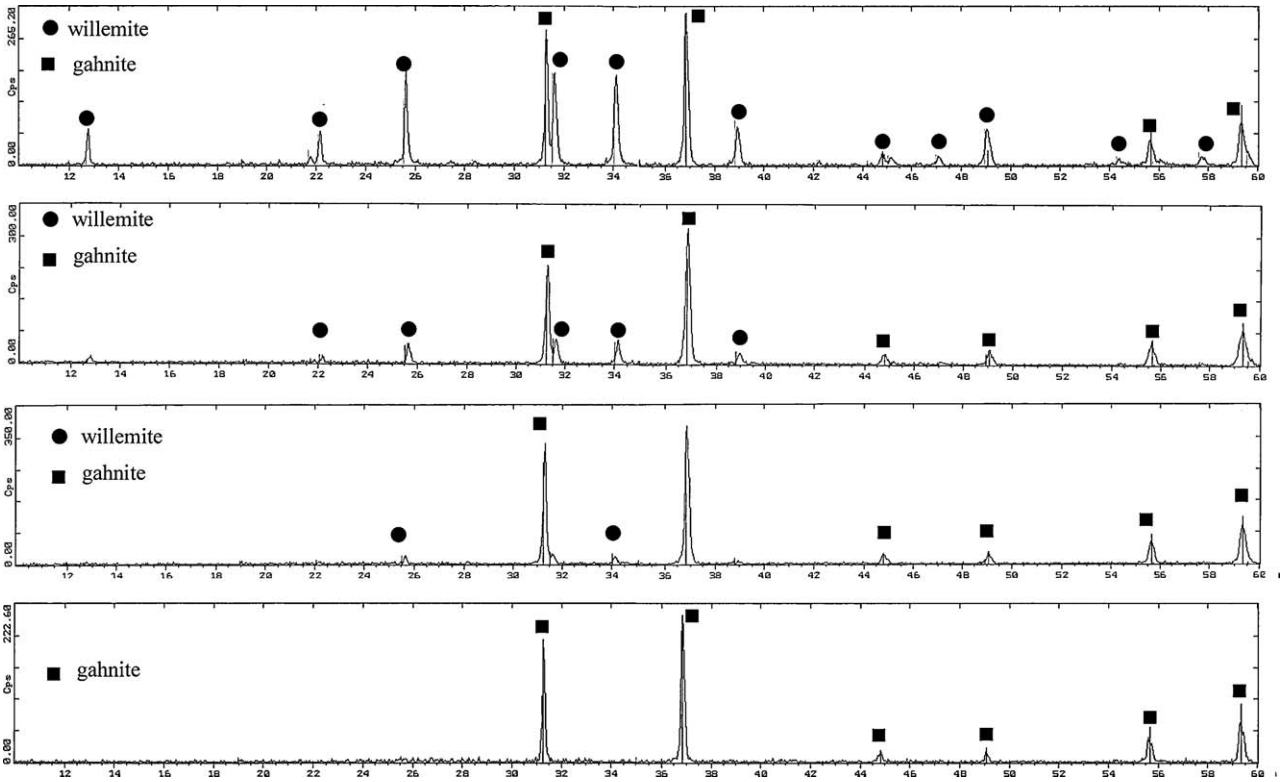

Fig. 4. Diffraction patterns of the specimens of the material: (a) heat treated at the temperature of the 1st peak of crystallisation, (b) at the temperature of the 2nd peak of crystallisation, (c) at the temperature of the first variant of the composite thermal treatment, where bond served as a function of the material, and (d) at the temperature of the second variant of the composite thermal treatment, where bond served as a function of the material.

is in a reasonable agreement with the investigations carried out by Adachi and Kato,[31–33] but according to them the wear rate was then higher. However, the precondition is the uniform structure of the material, i.e. with uniformly scattered crystals of a crystalline phase in a glasslike residue. The wear resistance of the materials under investigation remained within the range of $w_s = 10^{-4}$ mm^3/Nm, regardless of the type of the phases being present and the microstructure of the material. The higher value of w_s was assigned to the material undergoing heat treatment that effected in the formation of two different phases: of an island-silicate type (monoinosilicate) and a spinel type (Fig. 2).

A rise in the temperature of the heat treatment of the material in practice brings about a decay of willemite and makes it possible to obtain a uniform material with a phase of gahnite (Fig. 2c). This material undergoing heat treatment at 1100 °C, despite a larger size of gahnite crystals (1–5 μm) (Fig. 6c) compared to the size of crystals observed in material subjected to heat treatment at a maximum DTA peak temperature, i.e. 920 °C (1–3 μm) (Fig. 6b and c), was marked with a higher fracture toughness and a lower wear rate w_s (Fig. 5c, Table 2).

This is still a high wear resistance compared with the other group of glass-ceramics, e.g. the wear resistance of glass-ceramics with the addition of mica is relatively low; the values of the coefficients are fluctuating within 10^{-4}–10^{-1} mm^3/Nm.[34] Xiao et al.[8] tested wear on such materials, where diopside $CaMg(SiO_3)_2$ and wollastonite $Ca(SiO_3)_2$ was the main crystalline phase. In this system, a rise in the temperature contributed to the formation of the main crystalline phase in the form of diopside that is responsible for the mechanical strength and wear resistance. Despite the high hardness (9.52–12.35 GPa), the wear resistance within the temperatures from ambient to 500 °C was recorded at the level of 10^{-3} mm^3/Nm. Only a rise in the temperature, i.e. in the range of 500–800 °C caused the wear rate to decrease to 10^{-5} mm^3/Nm, mainly due to the ability to create the plastic deformation and in this connection an increase in the critical energy of micro-crack forming. The wear rate coefficient of the proposed glass-ceramics matters greatly in its application as a material bonding the abrasive grains and co-acting with these grains in the processes of material treatment.

Table 2
Specification of mechanical properties of material under investigations.

Type of a specimen	Hardness H_v [GPa]	K_{IC} [MPam$^{1/2}$]	w_s [mm^3/Nm]
Material A (880 °C)	6.86	1.65	1.43×10^{-4}
Material B (920 °C)	8.37	1.93	0.67×10^{-4}
Material C (1100 °C)	8.83	2.12	0.21×10^{-4}

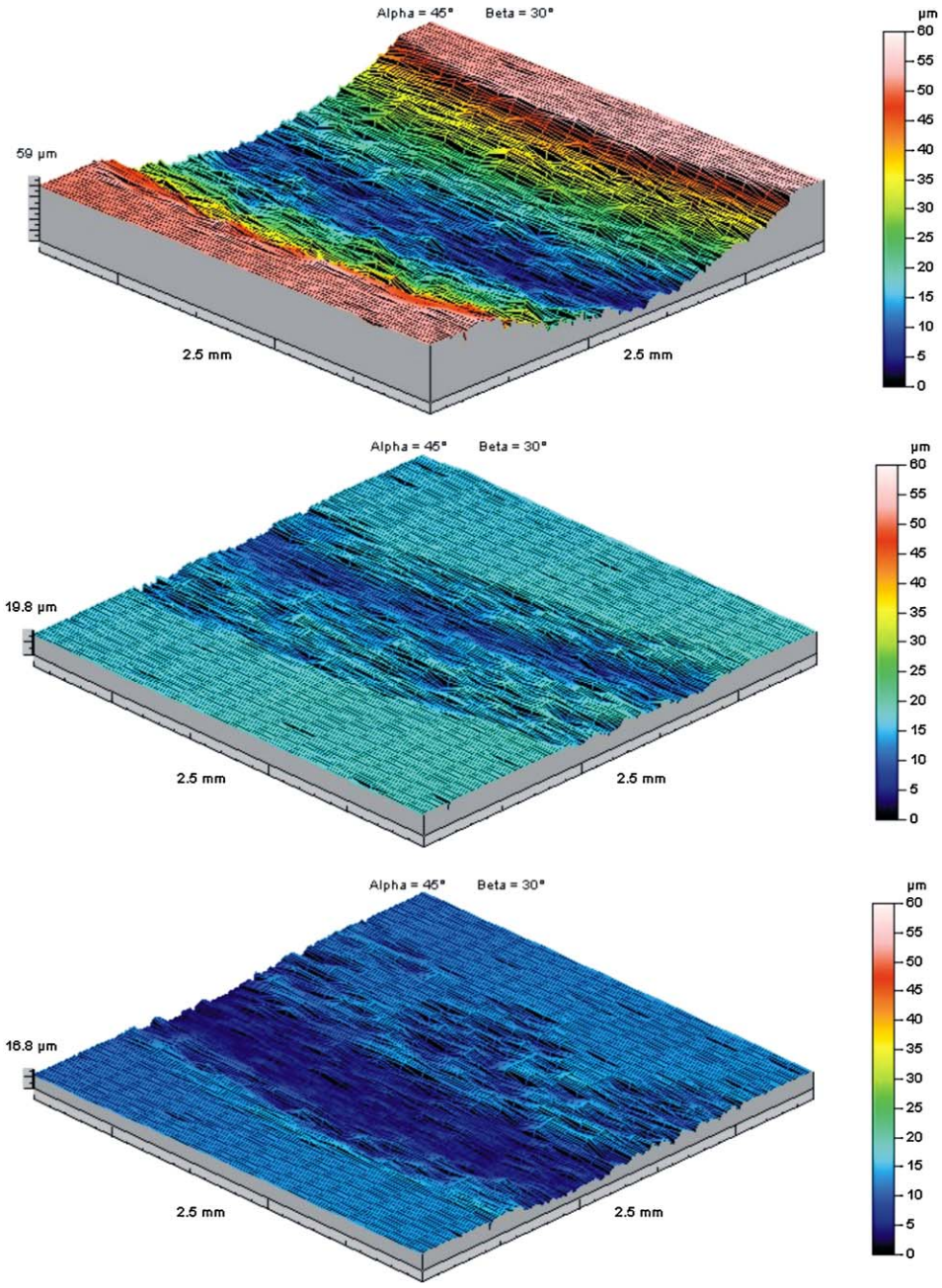

Fig. 5. 3D worn groove profiles of glass-ceramic specimens after different processes of heat treatment; (a) heat treatment at 880 °C for 2 h (of 1st crystallizing peak), (b) heat treatment at 920 °C for 2 h (of 2nd crystallizing peak), and (c) heat treatment at 1100 °C for 2 h.

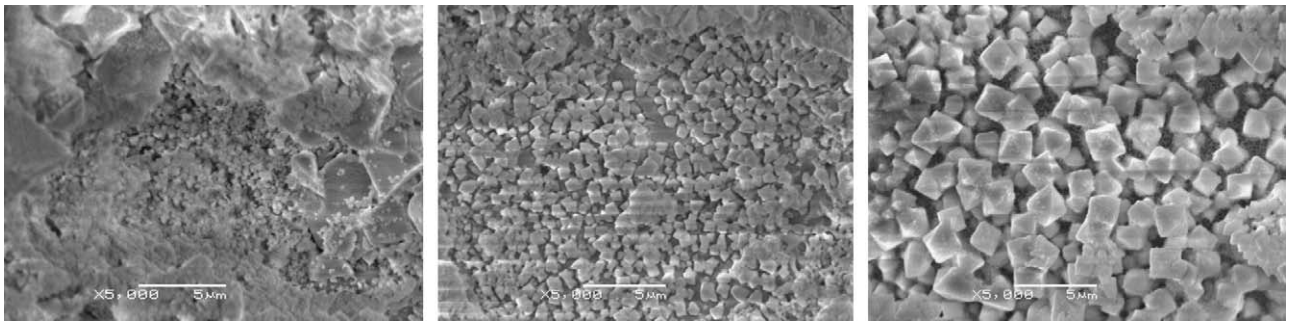

Fig. 6. Microstructure of material under investigation undergoing heat treatment for 2 h at temperatures: (a) 880 °C, (b) 920 °C, and (c) 1100 °C.

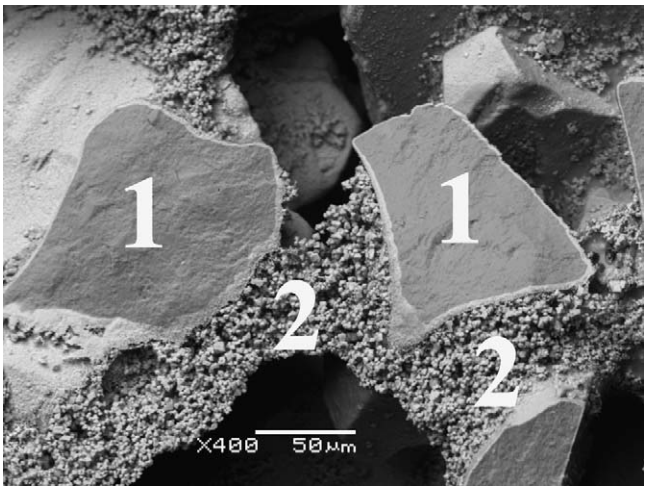

Fig. 7. Microstructure of a bond bridge made of proposed glass-ceramics in abrasive composite with Al_2O_3: 1 – abrasive grains of microcrystalline aluminium oxide, and 2 – glass-ceramic bridge with a gahnite phase.

A suitable heat-treatment of the composites including Al_2O_3 with an addition of such a material made it possible to obtain a uniform network of glass-ceramic bridges with a crystalline phase of gahnite uniformly distributed in a glass-like residue (Fig. 7). The application of such materials as binders should be taken into consideration in the future while designing the abrasive composites of a high strength and porosity.

4. Conclusions

In the proposed glass-crystalline material of $Al_{0.107}B_{0.374}Mg_{0.043}Zn_{0.282}Ca_{0.100}$ $Si_{0.927}O_3$ the formation of crystalline phases of gahnite and willemite required a similar thermal activation; the activation energies are $E_a = 325$ kJ/mol for willemite and $E_a = 314$ kJ/mol for gahnite, respectively. As a result of the heat treatment to 1000 °C, a two-phase material was obtained consisting of small crystals of gahnite (∼1 μm) and larger (∼5 μm) crystals of willemite. The presence of large crystals of willemite has an adverse effect on the mechanical properties of the material $w_s = 1.43 \times 10^{-4}$ mm^3/Nm, $K_{IC} = 1.65$ MPam$^{1/2}$. A rise in the temperature of the heat treatment above 1100 °C leads to a gradual decomposition of willemite, which makes it possible to obtain a glass-ceramic material with a homogeneous spinel phase GCS (Glass Ceramics Spinel) with the size of the crystallites from 1 to 5 μm. Owing to that, the fracture toughness and the resistance to an abrasive wear increases to $K_{IC} = 2.12$ MPam$^{1/2}$ and $w_s = 2.1 \times 10^{-5}$ mm^3/Nm, respectively, which significantly improves the relations among the coefficients: $K_{IC\ glass}/K_{IC\ SG} = 0.3$, $K_{IC\ GCS}/K_{IC\ SG} = 0.63$, $w_{s\ glass}/w_{s\ SG} = 1.34 \times 10^4$, $w_{s\ GCS}/w_{s\ SG} = 1.1 \times 10^2$, which provides an important step in the direction of optimisation. The use of GCS as a binder for abrasive grains of submicrocrystalline alumina allows the correct glass-crystalline network bridges to be obtained and therefore an increase in the wear resistance of abrasive composites with its participation is expected.

References

1. YektaEftekhari B, Alizadeh P, Rezazadeh L. Synthesis of glass-ceramic glazes in the ZnO-Al_2O_3-SiO_2-ZrO_2 system. *J Eur Ceram Soc* 2007;**27**:2311–5.
2. Chen GH, Liu XY. Sintering, crystallization and properties of MgO-Al_2O_3-SiO_2 system glass-ceramics containing ZnO. *J Alloys Compd* 2007;**431**:282–6.
3. Margha FH, Abdel-Hameed SAHM, Ghonim NAES, Ali SA, Kato S, Satokawa S, et al. Crystallization behaviour and hardness of glass ceramics rich in nanocrystals of ZrO_2. *Ceram Int* 2009;**35**:1133–7.
4. Salama SN, Darwish H, Abo-Mossallam HA. Crystallization and properties of glasses based on diopside-Ca-Tschermak's-fluorapatite system. *J Eur Ceram Soc* 2005;**25**:1133–42.
5. Wu Ch, Ramaswamy Y, Zreigat H. Porous diopside ($CaMgSi_2O_6$) scaffold: a promising bioactive material for bone tissue engineering. *Acta Biomater* 2010;**6**:2237–45.
6. Hu AM, Li M, Mao DL. Growth behavior, morphology and properties of lithium aluminosilicate glass ceramics with different amount of CaO, MgO and TiO_2 additive. *Ceram Int* 2008;**34**:1393–7.
7. Erol M, Genç A, Öveçoğlu ML, Yücelen E, Küçükbayrak S, Taptik Y. Characterization of a glass-ceramic produced from thermal power plant fly ashes. *J Eur Ceram Soc* 2000;**20**:2209–14.
8. Xiao H, Cheng Y, Yang Q, Senda T. Mechanical and tribological properties of calcia-magnesia-alumina-silica-based glass-ceramics prepared by in situ crystallization. *Mater Sci Eng A* 2006;**423**:170–4.
9. Park J, Oztruk A. Effect of TiO_2 addition on the crystallization and tribological properties of MgO-CaO-SiO_2-P_2O_5-F glasses. *Thermochim Acta* 2008;**470**(1–2):60–6.
10. Molla AR, Manoj Kumar BV, Basu B. Friction and wear mechanism of K_2O-B_2O_3-Al_2O_3-SiO_2-MgO-F glass-ceramics. *J Eur Ceram Soc* 2009;**29**:2481–9.
11. Schweiger M, Frank M, Cramer von Clausbruch S, Höland W, Rheinberger V. Microstructure and properties of a composite system for dental applications composed of glass-ceramics in the SiO_2-LiO_2-ZrO_2-P_2O_5 system and ZrO_2-ceramic (TZP). *J Mater Sci* 1999;**34**:3563–4572.
12. Liu C, Sun J, Zhang H, Ma Y, Qi N. Pressureless sintering of alumina matrix ceramic materials improved by Al-Ti-B master alloys and diopside. *Ceram Int* 2009:1327–33.
13. Wu Ch, Ramaswamy Y, Zreiqat H. Porous diopside ($CaMgSi_2O_6$) scaffold: a promising bioactive material for bone tissue engineering. *Acta Biomater* 2010;**6**:2237–45.
14. Junlong S, Changxia L, Xihua Z, Baowei W, Xiuying Ni. Effect of diopside addition on sintering and mechanical properties of alumina. *Ceram Int* 2009;**35**:1321–5.
15. Hitchiner MP, McSpadden SB. Evaluation of factors controlling cBN abrasive selection for vitrified bonded wheels. *Ann CIRP* 2005;**54**:277–80.
16. Jackson MJ, Mills B. Materials selection applied to vitrified alumina & cBN grinding wheels. *J Mater Process Technol* 2000;**108**:114–24.
17. Sunarto, Ichida Y. Creep feed profile grinding of Ni-based superalloys with ultrafine-polycrystalline cBN abrasive grits. *Precis Eng* 2001;**25**:274–83.
18. Pech M. Histoires de pores et de grains. *Mach Prod* 2005;**808**:33–4.
19. Beyer P. High-production grinding with vitrified bond superabrasives – HPB technology for vitrified bond cBN wheels. *Ind Diamond Rev* 2005;**65**:46–8.
20. Herman D, Krzos J. Influence of vitrified bond structure on radial wear of cBN grinding wheels. *J Mater Process Technol* 2009;**209**:5377–86.
21. Solozhenko VL, Dub NS, Novikov V. Mechanical properties of cubic BC_2N, a new superhard phase. *Diamond Relat Mater* 2010;**10**:2228–31.
22. Ichida Y. Mechanical properties and grinding performance of ultrafine-crystalline cBN abrasive grains. *Diamond Relat Mater* 2008;**17**:1791–5.
23. Li Z, Li Z, Zhang A, Zhu Y. Synthesis and two-step sintering behavior of sol–gel derived nanocrystalline corundum abrasives. *J Eur Ceram Soc* 2009;**29**:1337–45.
24. Walkowiak W, Herman D. Resistance to abrasive wear of glass-crystalline materials in relation to the sintered aluminum oxide. In: *Basics and Abra-*

sive Machining Technology. Publisher Division of Mechanical Engineering and Aeronautics at University of Rzeszow; 2007. p. 63–70.
25. Matusita K, Sakka S. Kinetic study on crystallization of glass by differential thermal analysis—criterion on application of Kissinger plot. *J Non-Cryst Sol* 1980;**38&39**:741–6.
26. Augis JA, Benett JE. Calculation of the Avrami parameters for heterogeneous solid state reactions using a modification of the Kissinger method. *J Therm Anal* 1978;**13**:283–92.
27. Lee YK, Choi SY. Controlled nucleation and crystallization in Fe_2O_3-CaO-SiO_2 glass. *J Mater Sci* 1997;**32**:431–6.
28. Lee SM, Kim SK, Yoo JW, Kim HT. Crystallization behavior and mechanical properties of porcelain bodies containing zinc oxide additions. *J Eur Ceram Soc* 2005;**25**:1829–34.
29. Tkalcec E, Kurajica S, Ivankovic H. Crystallization behavior and microstructure of powdered and bulk ZnO-Al_2O_3-SiO_2 glass-ceramics. *J Non-Cryst Sol* 2005;**351**:149–57.
30. Al-Harbi OA. Effect of different nucleation catalysts on the crystallization of Li_2O-ZnO-MgO-Al_2O_3-SiO_2 glasses. *Ceram Int* 2009;**35**:1121–8.
31. Kato K, Adachi K. Wear of advanced ceramics. *Wear* 2002;**253**:1097–104.
32. Adachi K, Kato K, Chen N. Wear map of ceramics. *Wear* 1997;**203–204**:291–301.
33. Adachi K, Kato K. Formation of smooth wear surfaces of alumina ceramics by embedding and tribo-sintering of fine wear particles. *Wear* 2000;**245**:84–91.
34. Nagarajan VS, Jahanmir S. The relationship between microstructure and wear of mica-containing glass-ceramics. *Wear* 1996;**200**:175–85.